

Microalgae bio-reactive façade: location and weather-based systematic optimization

Victor Pozzobon¹ 

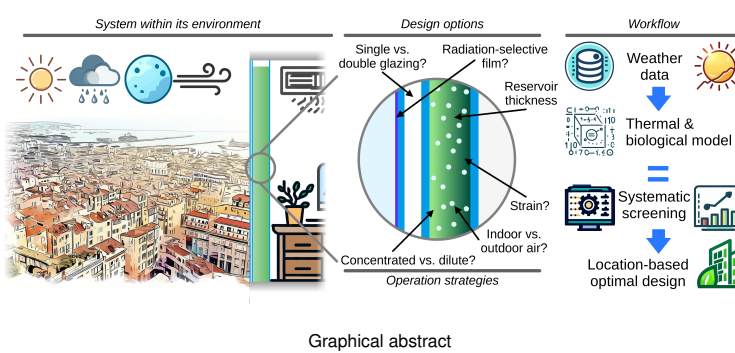
¹LGPM, CentraleSupélec, Université Paris-Saclay, SFR Condorcet FR CNRS 3417, Centre Européen de Biotechnologie et de Bioéconomie (CEBB), 3 rue des Rouges Terres 51110 Pomacle, France

This article explores the design of microalgae biofaçade thanks to a numerical model describing the system's thermal and biological behavior. Design options (single vs. double glazing, radiation-selective film, culture reservoir thickness) and operation strategies (light transmission, microalgae strain, sparged air origin, boiler fumes reuse) are screened systematically. The context for this investigation was the city of Marseille over a 10-year period (2013 to 2022) for which detailed meteorological data were available (air temperature, wind velocity and orientation, cloud cover, at a 3-hour resolution). These investigations revealed a very high level of interaction between the parameters (assessed by H² Friedman index), making the system notoriously complicated to design and optimize. Nevertheless, some conclusions can be drawn. In France, fitting double glazing equipped with a greenhouse radiation-selective film is essential to harness as much heat as possible (+16.7 % and +6.5 % of operation duration over year 2018, respectively). Similarly, a thermophilic strain is not relevant because overheating events are nonexistent in well-designed systems. Further refinements, such as the origin of the air blown into the culture reservoir and the reuse of combustion fumes from the boiler (+2.1 % performance), were evaluated from a technical point of view. However, their implementation would also be subjected to other considerations, such as the financial costs and environmental benefits. Finally, the model was applied to design the most efficient possible microalgae biofaçade system in the case of a hypothetical official building renovation.

has to be considerably lowered. Microalgae production technologies are often divided into two categories: open systems (such as raceway ponds) and closed systems (or photobioreactors). The first ones are inexpensive but have low productivity and high land requirement. Their modest performances can be explained by their ease of contamination and large volume, making them difficult to control (e.g., modifying the culture medium temperature, homogenizing nutrients, ...). On the contrary, closed systems are more compact, often well-instrumented, and highly controlled. Consequently, they are more productive and more expensive. A possible way to reduce their cost is to integrate photobioreactors into a host structure such as an office building. This type of implementation is called microalgae bio-reactive façades (or biofaçades, in short). It is regarded as part of a group of technological solutions leveraging the potential of the synergy between the host building and a biological system (3, 4). Indeed, combining the microalgal and advanced building technologies could bring benefits greater than the sum of each one taken individually. Integrating photobioreactors in a building could help reduce their costs by providing vertical support, utilities (water, thermal regulation, ...), and possibly nutrients (carbon dioxide recovered from the building, for example). On the building side, benefits could be shading, improved thermal comfort (by modulating incident heat better than glazing in summer), revenue generation, and aesthetic enhancements.

While this technology shows exciting potential, only a few authors have studied it. Among them, Pruvost *et al.* investigated *Chlorella vulgaris* culture in a biofaçade aiming at CO₂ biofixation. They led year-round tests to monitor performances and compare designs. For example, compared to a horizontal photobioreactor placed in the same conditions, a biofaçade allows for lower biomass productivity (7.68 vs. 8.84 g/m²/day). Still, this productivity exhibits smaller seasonal variation and is even stable from March to September. This finding suggests that a biofaçade would be easier to operate than its horizontal counterpart. In addition, the authors showed that the energetic relevance of such a system was conditioned to optimal thermal interaction with the building hosting it. Nevertheless, they also acknowledged that fine understanding and modeling of thermal integration was complex and laid outside of the scope of their work.

Going one step further, Barajas Ferreira *et al.* led an investigation of the relation between the design parameters (depth, width, ...) and the biomass productivity (5). They concluded that the optimal design would have a rather short depth (30



Microalgae | Biofaçade | Production | Optimization | Weather data
Correspondence: victor.pozzobon@centralesupelec.fr

1. Introduction

Microalgae are regarded as small biological factories capable of producing many molecules with applications ranging from food and feed to advanced compounds used in the cosmetic and pharmaceutical industries (1, 2). Still, before they realize the full extent of their promises, their production cost

mm) and narrow width (20 cm per compartment). Such a biofaçade would achieve a productivity of 10.5 g/m²/day of *Chlorella vulgaris* biomass. Finally, while not controlling it in their experiments, the authors also pointed out that temperature was a key factor driving the system's performance.

In their study, Umdu *et al.* acknowledged that thermal performances of a biofaçade are also a key parameter from a building efficiency perspective (6). As most of the thermal losses occur through the façade of a building, it is important to limit the system's overall thermal conductivity or U value. Yet, literature dealing with this aspect of biofaçade is limited. In an effort to fill this gap, Umdu's team led a systematic investigation of the geometrical parameters influencing the system's thermal behavior (reservoir depth, structural layer material and depth, air layer addition, and depth) (6). The authors concluded that PMMA (PolyMethyl MethAcrylate, a widespread polymer) should be preferred over glass as a glazing material to reduce building static load. Furthermore, the addition of a double-glazing dramatically cut the U value of the whole system (from 53 to 3 W/m²/K in the most favorable case). While absolute values can raise doubt, they nevertheless show that manipulating the biofaçade design is a potent tool to improve its thermal performance.

Expanding the scope of research further beyond technological considerations, two other reports are of note. The first is the work of Sarmadi *et al.*, who tackled the question of the visual comfort associated with microalgae biofaçade (7). Numerical tools were used to reproduce a modern office building with a mezzanine located in Tehran, serving as a test case. Acknowledging that visual comfort is a trade-off between sunlight availability and potentially blinding glare, the authors concluded that microalgae biofaçades are relevant in a sunny environment. Indeed, they efficiently reduce blinding glare intensity and occurrence. However, their usage as the sole glazing of a building is not advised as they could, in some configurations, create a too-dark environment leading to visual discomfort (8). Hence, they would have to be blended with conventional double-glazing. The second report of interest is the deployments of 185 m² of biofaçade in the BIQ house in Hamburg (9). The three main findings of this large-scale implementation were that the system achieved 4.4 % solar-to-biomass conversion efficiency, which compares well with laboratory studies on microalgae photoconversion efficiency (*e.g.*, 5.01 % (10), 5.65 % (11), or 4.34 % (12)) and 21 % thermal energy recovery efficiency. These figures highlight the biotechnological and thermal relevance of the system. Moreover, the tests again highlighted the crucial role of temperature on *Chlorella vulgaris* growth, hence system performances. Finally, this field deployment demonstrated especially good social acceptance of the technology, which could be further reinforced by the recent proposition of a multicolor biofaçade made of several compartments hosting microalgal species of different color (8).

In all the studies above, scholars emphasized the pivotal role of the thermal management of the system, either from a building or biological perspective. Yet, knowing the thermal behavior of a biofaçade is complex as it results from:

- Direct incident illumination from the sun, which provides both heat and the photosynthetically active radiation required for the microalgae to grow,
- Radiative heat exchange with the sky, which also provides photosynthetically active and thermal radiation but can also cool the system down, especially at night,
- Radiative heat exchange with the surrounding (buildings, fields, ... depending on the location),
- Convective heat exchange with the outdoor air,
- Radiative and convective exchange with the building hosting the biofaçade,
- Heat supplied and removed by the gas flow sparging within the culture medium.

In addition to the diversity of the heat exchange phenomena at stake, they have to be considered in conjunction with day/night and annual cycles, as well as meteorological conditions. Modeling their interplay at a sub-hour resolution and assessing the associated biotechnological performances is a challenge that was addressed in a companion article. The present article intends to apply this biology-coupled convective-radiative model to evaluate the effect of several design and operating conditions choices on the overall performance of the system. Thanks to the versatility of the model, numerous options could be investigated in a systematic manner: single vs. double-glazing configuration, application of radiation-selective films, building boiler fumes reuse, ... The primary outcome of this work is the identification of the combination of microalgae biofaçade design and operating procedures maximizing microalgae production for a given building implementation (location, orientation, weather conditions). The secondary outcome is the relative importance of each parameter, allowing one to rank them by order of relevance when designing a system and decide upon their benefit/cost ratios. Tertiary, taking advantage of the French weather agency's open data policy, realistic meteorological conditions could be simulated over several years, providing valuable estimates of potential year-to-year variation. Hence, this work paves the way to location-specific best-achievable performance prediction, thus advising on the economic and environmental relevance of a microalgae biofaçade deployment.

2. System, models and performance indicators

2.1. Considered system

Figure 1 presents a schematic representation of the considered microalgae biofaçade and some possible design variations. Furthermore, the graphical abstract illustrates the interaction of a biofaçade model within its environment. The core of the system is a reservoir hosting the microalgae culture. This reservoir is held by two layers of PMMA and features some gas spargers at the bottom and a vent at the top.

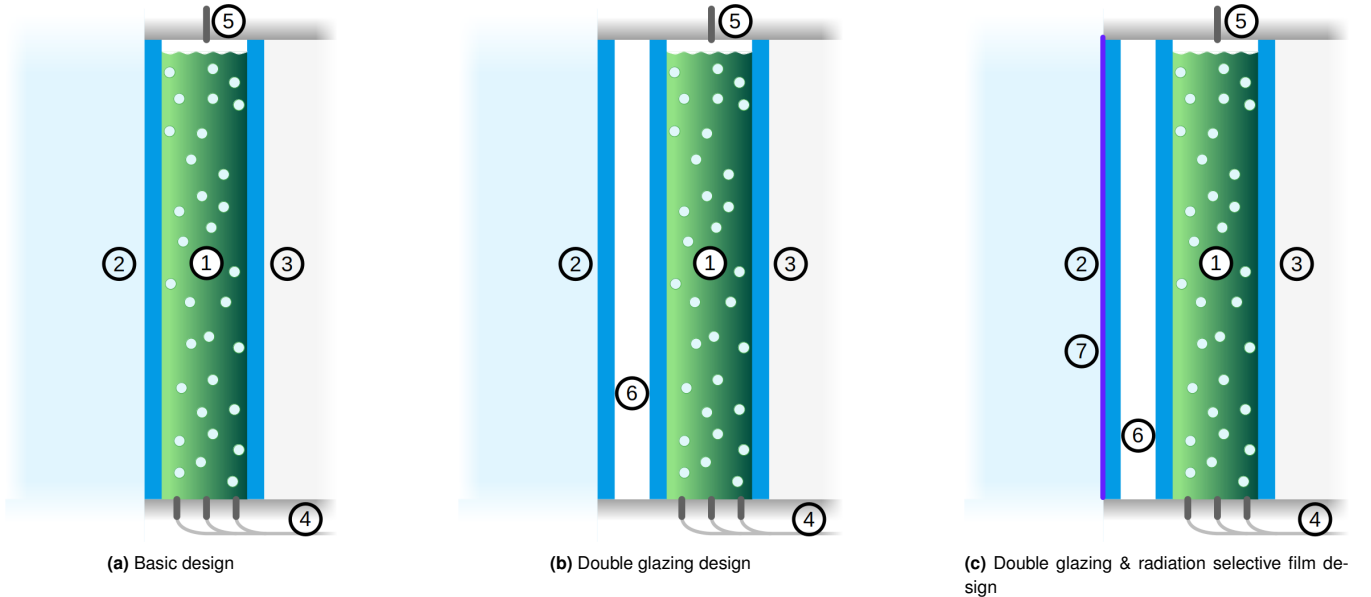


Fig. 1. Schematic representation of possible microalgae biofaçade designs. 1 - microalgae culture reservoir, 2 - outward PMMA layer, 3 - inward PMMA layer, 4 - gas sparging system, 5 - vent, 6 - double glazing, 7 - radiation-selective film

The typical geometry of the system is 1 m in width and 4 m in height (standard floor height in office buildings). Its thickness is variable depending on design choices. Furthermore, the system is considered integrated into an office building façade at a height somewhat higher than the surrounding building (about 20-meter high) to ensure adequate sunlight access. Finally, it is placed in the middle of the façade, to ease the considerations about outdoor convective heat transfer induced by the wind (13).

2.2. Thermal model

The model describing the thermal behavior of the biofaçade is presented, validated, and analyzed in detail in the companion article and summarized in the Supplementary Materials. In a nutshell, the model sums the absorbed and emitted convective-radiative heat fluxes to compute the evolution of the microalgae reservoir temperature (Fig. 2). The considered heat fluxes are:

- incident direct sunlight, Φ_{Sun} which is divided into visible and infrared radiation,
 - incident and emitted radiation towards the sky, Φ_{Sky} ,
 - incident and emitted radiation towards the surroundings, Φ_{Sur} ,
 - incident and emitted radiation towards the host building indoor, $\Phi_{In,Rad}$,
 - convective-conductive exchange with the outdoor air, $\Phi_{Out,Conv}$,
 - convective-conductive exchange with the indoor air, $\Phi_{In,Conv}$,
 - heat inflow from the sparged gas, $\Phi_{Gas,Inlet}$, and heat outflow from the vented gas, $\Phi_{Gas,Outlet}$.

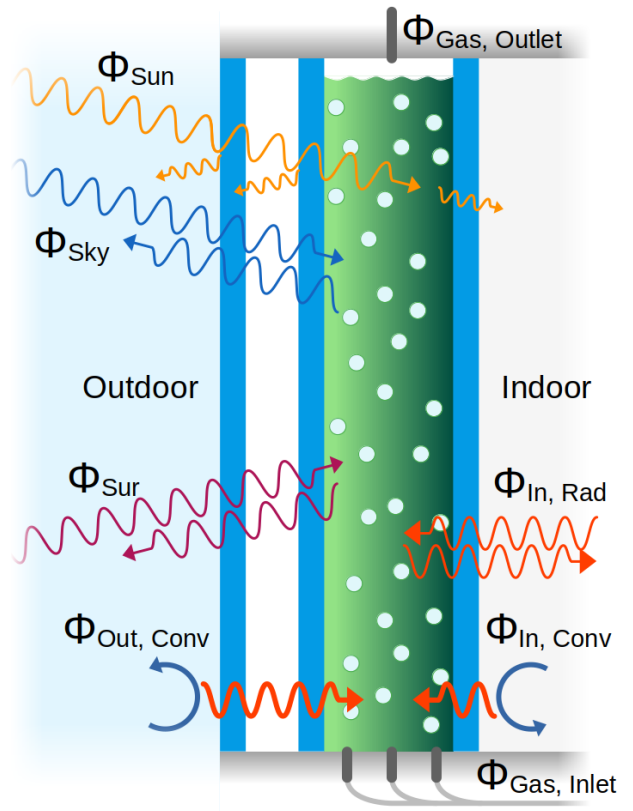


Fig. 2. Schematic representation of the considered microalgae biofaçade, featuring double glazing, but no radiation-selective film. The reported heat fluxes (Φ) are introduced in the text

Conductive heat fluxes in the PMMA and stagnant air layers are described using resistance in series model. Convective exchanges are modeled using correlations established from experimental data. Furthermore, solar illumination is described by the model proposed by the Illuminating Engineering Society, based on solar time, position on Earth, cloud cover, and orientation (14). Finally, as little is known about radiative exchanges with the surroundings, they are modeled using the Stefan-Boltzmann formula weighted by relevant view factors and emissivities.

2.3. Biological model

When it comes to biofaçade performances, scholars emphasized the pivotal role of the temperature of the system. Indeed, microalgae are cells of a few micrometers in diameter and incapable of regulating their temperature. Their inability to manipulate their temperature is all the more detrimental as this parameter is key to their bloom or collapse. Indeed, it controls, among others, enzymes' reaction rates and affinities. High temperatures (above 45 °C for mesophilic species, 55-60 °C for extremely tolerant microalgae) can even denature protein and DNA irreversibly (15). On the contrary, freezing temperatures can induce the growth of large ice crystals within the cells, lethally damaging them (16).

The impact of temperature on microalgae growth can be modeled using the Cardinal Temperature Model with Inflection (17). It allows drawing three qualitative temperature ranges (Fig. 3). The first one, in blue, is deemed too cold as the growth rate is below 75 % of the optimal value. The second one, in green, is considered adequate. The last one, in red, is flagged as dangerous as the growth rate drops below 75 % of the optimal value because of overheating. Finally, one last range of temperature was considered in this work as it is also dangerous to the system and induces a fatality to the cells: the sub-zero condition. A careful observer would note that both strains exemplified in Figure 3 (detailed afterward) belong to the *Chlorella* genus. Indeed, this genus was chosen as it is commonly encountered in both industrial and scientific communities, is approved as food and feed by (EFSA - Ares (2022) 1668627 - and US FDA - GRN 00396 -), and features a sizable biotechnological potential (18).

In addition to temperature, light is a crucial parameter to account for as it drives photosynthesis, hence the system's productivity. The incident light is obtained by summing the one coming directly from the sun and the one coming from the sky. Yet, the incident light is not the most relevant indicator of the ability of microalgae to grow. Indeed, even if the incident light is high enough to power photosynthesis, it can quickly become insufficient over a large part of the biofaçade because of cell light absorption. Therefore, the volume-averaged illumination over the depth of the culture reservoir was chosen as the indicator of the adequacy between incident light and biological needs. In accordance with several reports for *Chlorella vulgaris* cultures in tightly controlled light condition (19, 20), a threshold value of 150 $\mu\text{molPhotonPAR/m}^2/\text{s}$ was retained. Below this value, the culture is considered light-deficient. Above, it is consid-

ered light-sufficient. The two last questions that can come to the reader's mind are the intermittency of the light experienced by the cells and a potential excess of light. As for the first one, cells will be shuttled from light to dark zones, and vice-versa, by the fluid flow. Therefore, they will experience rapid light/dark cycles. Yet, recent work showed that their physiological response to such cycles is not different from the one under continuous light, at least up to 800 $\mu\text{molPhotonPAR/m}^2/\text{s}$ (20). Furthermore, when adequately cycled between light and dark zone (as in this system), cells can handle illumination up to 7000 $\mu\text{molPhotonPAR/m}^2/\text{s}$, corresponding to 3.5 times the illumination at midday in summer, which is quite unlikely to occur naturally (21). Those two last concerns can therefore be ruled out.

Finally, one should note that additional factors other than temperature and light would influence microalgal growth in actual culture conditions: pH, culture medium composition, and shear stress experienced by the cells, ... For the sake of simplicity, they were considered to be controlled within adequate range for microalgae cultivation. Similarly, as the culture grows, its optical thickness will increase and modulate the overall biofaçade performances. Therefore, for the sake of simplicity, again, the culture is assumed to be monitored by an inline transmitted light sensor, which orders dilution to keep the culture density at the desired value.

2.4. Weather data

The meteorological data powering the model was obtained from Météo-France (the public French weather forecast agency). The whole set covers France, with about one station per administrative region. Data span from 1996 to date, with a measurement every 3 hours. The reported parameters are numerous. The ones used for this work are air temperature, cloud cover, wind velocity (at 10 m above the ground), wind direction, relative humidity, and static pressure. The database was accessed on April 2023.

Among the possible spatial locations and time spans, the years 2013 to 2022 in Marseille and Paris, France, were chosen for demonstration. Three reasons pointed toward these choices. First, a 10-year span was deemed long enough to assess inter-annum variation. Second, Marseille is a city located in the south of France, where solar resource is abundant. Paris is a somewhat more northern city featuring tall buildings (hence numerous potential spots for biofaçade installation). However, the temperature and solar resources will be lower than the ones in Marseille. This contrast was sought to highlight how different optimal microalgae biofaçade designs would be at the two locations. Third, the year 2013 was the last year featuring a thermal history resembling the 1950-1990 period (it would have been considered hot, but not unlikely hot), and the year 2022 was the hottest ever reported. Again, the contrast was sought to assess biofaçade performance under the most diverse conditions possible.

2.5. Performance indicator and numerical details

While the model delivers results allowing to compute the biofaçade temperature and internal illumination with a sub-

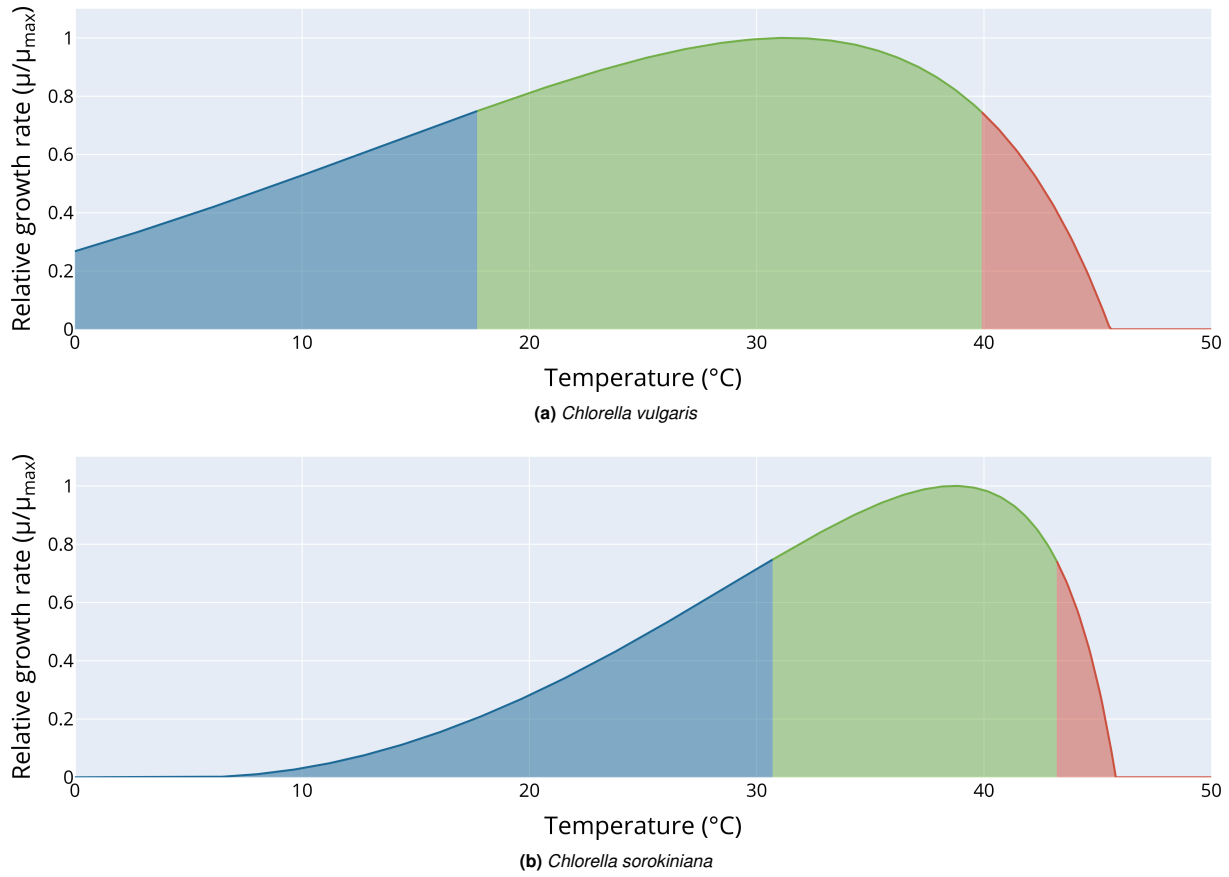


Fig. 3. Relative growth rate of the two *Chlorella* strains as a function of temperature

hourly resolution, manipulating this tremendous amount of data would hamper the analysis of the differences between the tested configurations. Therefore, synthetic indicators have been preferred. To elaborate them, the daytime operation (solar altitude above 0°) has been divided into six categories: (light-deficient or light-sufficient) × (too-cold, adequate, or too-hot temperature). Potentially freezing temperatures (during the winter nights) were also tracked over daytime and nighttime as they would induce an additional operational constraint. Furthermore, the first and tenth deciles (and their spreads) of the microalgae culture temperature distribution are also considered valuable indicators as they provide information on the occurrence and intensity of extreme events. To ease their assessment and interpretation, these indicators are reported graphically, as exemplified in Figure 5 (Top left) for the reference configuration over the year 2013 in Marseille. Among the different indicators, the most important is the number of hours during which the biofaçade features adequate temperature and sufficient lighting. Hence it will be the one extensively discussed hereinafter. From a mathematical point of view, this condition is marked τ and defined in Eq. 1:

$$\tau = \sum_i^n ((T_{low} < T_i < T_{high}) \times (\bar{I}_i > 150 \mu\text{mol Photon/m}^2/\text{s})) dt \quad (1)$$

where i is a running index, n the number of timesteps (dt) covering the period of interest (e.g., the year 2018 or ten years, ...), T_i the biofaçade temperature at a given time, T_{low} and T_{high} the lower and upper values of the temperature range allowing microalgae adequately (strain-dependent, see Subsection 3.6), and \bar{I}_i the volume averaged illumination within the system at a given time.

In addition to the absolute values of performance indicators, such as the ones illustrated in Figure 5, assessing the associated confidence level is important. In the case of a microalgae biofaçade, uncertainty can originate from two sources.

The first one is a year-to-year variation. Indeed, weather conditions are not identical from one year to the other. As a biofocade is obviously exposed to meteorological conditions, changes in air temperature, cloud cover, wind velocity, ... modulate its thermal behavior. This problem could be circumvented by using Typical Meteorological Year, a tool generating weather-realistic meteorological data based on the location (22). However, some limitations exist. For example, the generated data might be somewhat inaccurate in coastal areas or when available meteorological stations are far away from the location of interest. In this work, having access to the large dataset from the French weather forecast agency, it was chosen to rely on actual weather data recorded over the past ten years to assess the magnitude of year-to-year variation.

The second source of variability is the uncertainty sur-

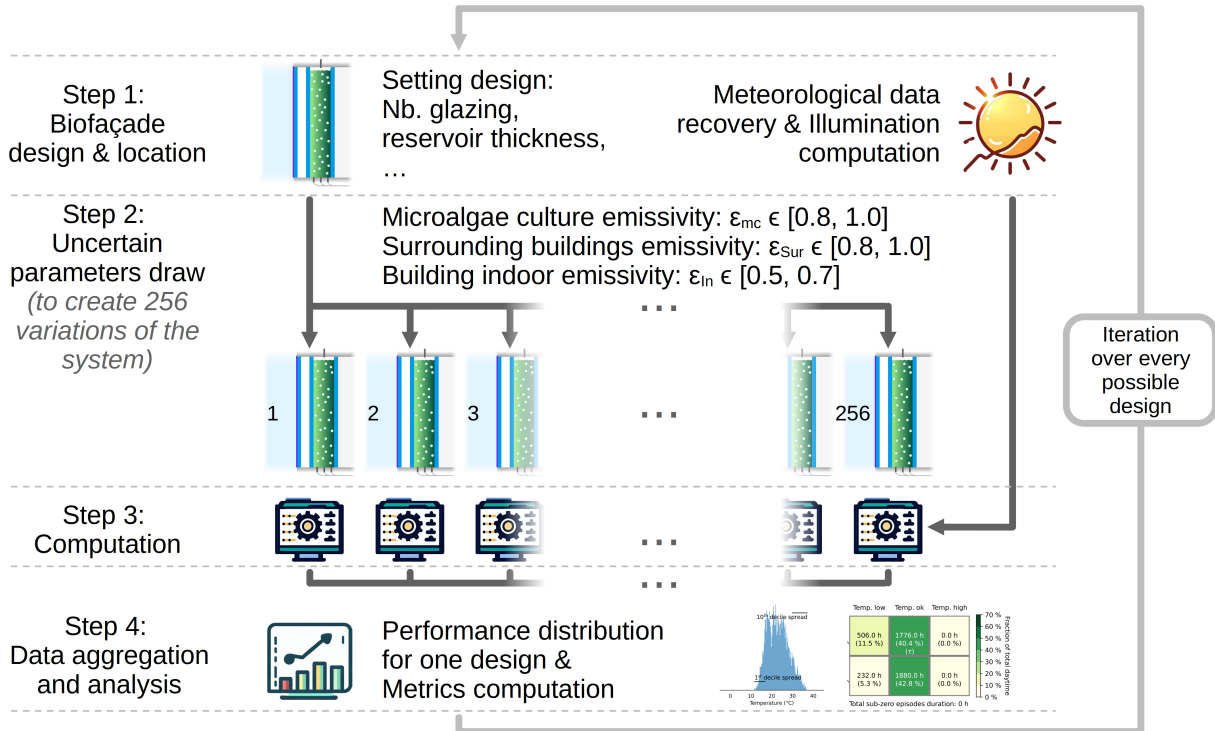


Fig. 4. Numerical workflow deployed to screen every possible configuration while taking into account the variability originating from uncertain parameters

rounding the value of some physical parameters. More specifically, in the companion paper, a global sensitivity analysis showed that the microalgae culture emissivity and the building indoor emissivity are the parameters inducing most of this type of variability. Surrounding emissivity was also demonstrated to be a possible modulator in some cases. Therefore, to account for it, a Monte Carlo approach was adopted. For each configuration, the model was run several times with values of microalgae culture emissivity ($\epsilon_{mc,max}$), building indoor emissivity (ϵ_{In}), and surrounding emissivity (ϵ_{Sur}) drawn from a uniform distribution (between 0.8 and 1.0, 0.5 and 0.7, and 0.8 and 1.0, respectively). Thus a distribution of performances was obtained. From it, the average performances and the associated standard deviations were extracted. To ensure efficient convergence, the values were drawn following a Sobol's sequence (a pattern design to explore hypercubes uniformly in such a way that integrals converge rapidly and accurately while minimizing mesh generation computer load)(23). One should note that using this type of sequence is particularly conservative as extreme configurations are as likely to be selected as central ones. Therefore, it ensures the robustness of the conclusions drawn. A convergence analysis (graphed in the Supplementary Materials) showed that 256 draws were enough to yield stable estimates of averages and standard deviations for all the aforementioned indicators.

Finally, the whole numerical process is presented graphically in Figure 4.

3. Tested scenarii

Once the model and the data have been secured, the question of the parameters to explore arises. The key design pa-

rameters and operating procedures envisioned in a biofaçade design process are presented in Table 1 (reference case and the varied parameters). For an extensive description of the parameters used in the model and the associated values, the reader is kindly referred to the companion article. The following Section details the rationale behind the investigation of these parameters.

3.1. Single vs. double glazing

Among the possible evolutions from the system's reference configuration, double-glazing is the most obvious one (6). By fitting externally an additional layer of PMMA, trapping 1.5 cm of stagnant air, one can expect to retain more heat within the system. This additional heat is expected to help increase the fraction of time the biofaçade operates in the thermally adequate range while lowering the amount of captured visible radiation. Still, the system may also become prone to overheating in summer. The relevance is, therefore, to be evaluated with respect to the biological capabilities. Furthermore, adding a PMMA layer will also lower the U-value of the system and increase its building-wise thermal performance. Thinking further ahead in terms of glazing, one could also think of integrating the microalgae culture system into a double skin façade which offers additional means to act on the system temperature (24, 25). While of great interest, this glazing configuration was excluded from this analysis for the sake of simplicity.

3.2. Radiation-selective films

Another refinement that could help to manage a microalgae culture better is the use of spectrally selective film. From a technical perspective, this type of film could be easily applied

Design parameters and operating procedures	Reference value	Variation	Unit
Elevation of the biofaçade above the ground	20	-	m
Width of the biofaçade	1	-	m
Height of the biofaçade	4	-	m
Thickness of the biofaçade reservoir (e_{mc})	0.05	0.02 and 0.08	m
Number of outdoor glazing	1	2	-
Green light transmitted fraction (α)	0.5	0.25 and 0.75	-
Sparged gas origin	Building	Outdoor	-
Use of boiler fumes	No	Yes	-
Orientation	South	East, Southeast, Southwest, and West	-
Strain type	Regular	Thermophilic	-
Radiation-selective film	None	Greenhouse and Visible-only	-

Table 1. Key geometrical, physical and biological parameters describing the reference case

to the external glazing of the microalgae biofaçade, making them valid options to explore. The idea of manipulating the light spectrum to better control microalgae growth can be applied with two goals in mind:

- adjusting the thermal/photosynthetic radiation ratio (to increase heat capture in cold environments or prevent overheating in hot ones) to foster growth (26),
- blocking photosynthetic radiation while capturing heat (in a swimming pool, for example) to prevent microalgae proliferation (27).

The first option is of interest for a microalgae biofaçade. In the case of a cold environment, Balocco *et al.* proposed a 200 µm film blocking long-wavelength radiation in a greenhouse (transmittance of 26.22 % for ultra-violets, 89.15 % for the visible spectrum, 83.15 % for the near-infrared, and 51.14 % for the medium and long infrared) (28). The aim was to capture as much heat and photosynthetically active radiation as possible while limiting reemission. In the case of a hot environment, Gao *et al.* developed a titanium oxide film of 76 µm film doped with niobium and fluorine (transmittance of 76.4 % for the visible spectrum and 42.9 % for the infrared) (29). The aim was to limit thermal radiation while harnessing visible light. The potential use of these films was implemented by multiplying the respective radiative fluxes in the model (visible, near infrared from the sun or long wavelength infrared emitted by the surrounding and the culture) by the transmittances reported by the authors.

3.3. Microalgal culture density

Another modulation that can be included in the design strategy is the cell concentration of the culture hosted by the biofaçade. A higher concentration would be beneficial from a process point of view. Indeed, high-concentration cultures are easier to harvest (30). Furthermore, if dense enough, it can open the way for wet biomass downstream processing, which overcomes the need and cost of biomass drying. Nevertheless, increasing the biomass concentration increases the heat captured by the culture and potentially reduces visual comfort within the host building (by reducing the luminosity) (8). Therefore, the pros and cons have to be weighed against the magnitude of the impact of this design parameter (7).

Still, one should note that the culture concentration alone is a poor design parameter. Indeed, it strongly correlates with the culture compartment thickness, as they form the optical thickness together. Therefore, to disambiguate the coupling between the two parameters, cell culture density is approached by considering the amount of light passing through the culture (α parameter), which is equivalent to the culture's optical thickness. Furthermore, from a practical perspective, as biofaçade are intended to be installed in building hosting human activity, visual comfort (light passing through) would surely be preferred to cell concentration as a design parameter. In this work, the reference value was chosen at 50 %. Two others were added for the systematic screening: 25 % (higher cell density) and 75 % (lower cell density).

3.4. Microalgal reservoir thickness

The previous section introduced the importance of illumination management by manipulating cell concentration. Another option would have been to tune the reservoir thickness while maintaining the cell concentration constant. Still, this would have had two combined effects: changing the amount of absorbed energy and modifying the system's thermal inertia (dominated by the mass of water within the reservoir). Luckily, it is possible to uncouple the two effects by using the optical thickness as a design parameter (as suggested in the previous Section). Therefore, changing the reservoir thickness while maintaining the optical thickness (by modulating concentration) would only affect the thermal inertia of the biofaçade.

Increasing the thermal inertia seems a relevant idea to limit acute hot events and manage transient cloud cover (lowering incident heat) during the mid-season. Yet, it will be at the price of an increased structural load for the host building. Thus, the choice has to be made with care. In this view, three thicknesses were tested: 2, 5, and 8 cm.

3.5. Sparged gas

In the companion article, the contribution of the sparged gas to the total thermal balance of the system was shown to be modest. Yet, from an environmental perspective, it seems relevant to investigate at least three strategies, which could, in part, contribute to CO₂ fixation (31). The first one is sparging air from the building to minimize the air pollution it emits.

This configuration is the reference case. The second strategy would be to sparge air coming from the outdoors. This time, the biofaçade would actively contribute to reducing urban air pollution. From a modeling perspective, it implies that the sparged air inlet temperature would not be equal to the one of the host building but the one of the outdoor air. A last strategy would be to inject fumes from the boiler powering the building's heating system during winter. This way, one would valorize both waste heat (fume temperature around 153 °C (32)) and CO₂ (7.2 % content in the fumes (32)) coming from the boiler. From a technical perspective, the fumes would be channeled to the biofaçade and diluted (by a factor 4, in the present work) before injection. From a biological perspective, this operating procedure is made possible by the high CO₂ tolerance observed for microalgae of the *Chlorella* genus (up to 40 % for certain species (33)). This strategy can be employed as a modulation of the two previous ones. Numerically, it is described increasing in the sparged air temperature, according to the dilution rate, from the beginning of November until the end of March.

3.6. Thermophilic microalgae strain

Up to this point, only thermal options have been considered to enhance microalgae biofaçade performance. However, a biological option exists to mitigate the negative impact of high-temperature events: opting for a microalga tolerating this type of event. While numerous thermophilic strains exist, *Chlorella sorokiniana* was chosen here. Indeed, as a member of the *Chlorella* genus, it can be valorized in the same manner as *Chlorella vulgaris*. Hence, this strain would not perturb the produced biomass valorization workflow (food, feed, pigment production, ...) following its production within a biofaçade. From a numerical standpoint, experimental data were used to parametrize two instances of the Cardinal Temperature Model with Inflection. Figure 3 presents the growth rate dependence upon the temperature of the regular strain (*Chlorella vulgaris* (34)) and the thermophilic one (*Chlorella sorokiniana* (35)). As one can see, the thermophilic strain has a narrower range of adequate temperature (from 30.6 to 43.2 °C, compared to 17.7 to 39.9 °C for the regular strain). Yet, it featured an extension of the upper value of the range by +3 °C. Therefore a trade-off can be expected between managing acute hot events and nominal conditions production. While it may not seem evident for locations in a temperate climate, such as France, this option could be very relevant to cultivate microalgae closer to the equator or under a Mediterranean climate.

3.7. Orientation

The last design parameter explored in this work is the biofaçade orientation. Indeed, as the system features intrinsic (from water mass) and extrinsic (surrounding environment temperature dynamic) thermal inertia, there may be better performing orientation than a plain South orientation (36). Hence several orientations of the biofaçade were tested. In addition to consideration of sole performance, in actual cases, the orientation of the biofaçade will be imposed by the host

building architecture and, therefore, not chosen according to thermal/biological optimality. Thus, exploring a priori under-performing orientation (e.g., due East) is also necessary. This way, the reported performances will help decide whether it is relevant to set up a microalgae biofaçade in this direction if given the opportunity.

4. Results and discussion

Altogether, the tested combinations and the associated uncertainty estimation sum up to about 11 million individual runs. The model was able to simulate them all over the chosen ten-year span. Given the tremendous amount of data it represents, the different scenarii will be examined in a progressive manner. First, the focus will be set on the best-performing configuration. Its performances will be dissected to understand which parameters support its sizable increase in performance with respect to the reference case. Second, the parameters' main effects and interactions will be investigated. Third, the impact of the host building location will be assessed by comparing Paris and Marseille scenarii. One should note that the massive data generation procedure described earlier has an impact on the way data have to be processed. Indeed, while the statical variations induced by using Sobol's sequence could technically be analyzed using the ANOVA framework, the high number of samples makes this approach irrelevant (37) as all differences appear statistically significant. Therefore, effect size, effect size indices (such as Cohen's d (37, 38)), and interaction indices (such as Friedman's H² (39)) will be used to drive the analysis. Cohen's d provides a comparison of two populations' means, taking into account their standard deviations (Eq. 2). In terms of interpretation, an absolute Cohen's d value of 0.2 is deemed minor, 0.5 medium, and large above 0.8. Friedman's H evaluates the amount of variance tied to the interaction of a parameter with the others (either in sets or a whole). To do so, it subtracts from the whole effect of a combination of variables the main effects of the individual variables. Therefore, the remaining contribution originates from their interaction (Eq. 3). This value is then normalized by the overall variation to yield an indicator between 0 and 1. A H² value of 0.1 is considered substantial, while a value above 0.25 is classified as heavy. This metric can be used in various scientific field to rule out potential interaction between parameters (for very low values, in the context of fish population spatial distribution (40), for example) and underline their relevance of coupled effect (for large values, in the context of fungal disease spreading in coffee plantation (41), for example).

$$d = \frac{\bar{X}_1 - \bar{X}_2}{\sqrt{\frac{s_1^2 + s_2^2}{2}}} \quad (2)$$

$$H_{j,k}^2 = \frac{\sum_{i=1}^N (\hat{F}_{jk}(x_{i,j}, x_{i,k}) - \hat{F}_j(x_{i,j}) - \hat{F}_k(x_{i,k}))^2}{\sum_{i=1}^N \hat{F}_{jk}^2(x_{i,j}, x_{i,k})} \quad (3)$$

where, x_j and x_k are variables, \hat{F} the regression model

Design parameters and operating procedures	Reference configuration	Best configuration	Marginal contribution	Basal contribution		
			10-year average effect size (h)	10-year averaged Cohen's d index	10-year average effect size (h)	10-year averaged Cohen's d index
Thickness of the biofaçade reservoir (ϵ_{mc})	0.05	0.08	133	0.964	-109.9	-0.36
Number of outdoor glazing	1	2	384.9	1.931	38.96	0.083
Green light transmitted fraction (α)	0.5	0.75	216.8	1.478	37.19	0.164
Sparged gas origin	Building	Building	-	-	-	-
Use of boiler fume	No	Yes	81.95	0.326	24.75	0.125
Orientation	South	South	-	-	-	-
Strain type	Regular	Regular	-	-	-	-
Radiative film type	None	Greenhouse	208.3	0.461	46.63	0.084

Table 2. Reference and best configuration design parameters with associated marginal and basal effect size and effect size indices

outcome and i the index representing the data point.

4.1. Reference vs. best configuration

The first question one might naturally ask is: which configuration is the best? Yet, this raises the question of how to define optimality. In our case, optimality was defined as the highest amount of production while keeping to 0 the number of sub-zero and overheating episodes. This way, the configuration would ensure both efficient production and robust operation. Considering these criteria, among all the simulated configurations, the best one was identified as a south-facing biofaçade fitted with double glazing and a greenhouse radiation-selective film. The sparged air would come from the building, and part of the boiler fumes would be redirected to the biofaçade during winter. It would host a dilute culture of *Chlorella vulgaris* (the regular strain) in an 8 cm thick reservoir (Tab. 2). On average, over the 10 tested years, this configuration would be able to create adequate temperature and illumination for microalgae growth during 2247.6 ± 313.6 h per year, versus 1717.6 ± 292.9 h for the reference setup. This represents a sizable 31 % increase.

Going further into details, Figure 5 presents the thermal history distributions as well as the performance indicators for the reference and the best systems for the year 2013 (the last of the not abnormally hot years) and 2022 (especially hot year). As one can see, the best configuration displays a much narrower temperature distribution with a higher average. During a regular year, as in 2013, the optimized system increases the total duration spent with adequate temperature by 66 %. During a hot year, such as 2022, this increase is reduced to +38 %. Interestingly, the capacity of the system to harness more heat did not make it enter an overheating episode, undoubtedly because of the higher thermal inertia offered by the reservoir thickness increase from 5 to 8 cm. Regarding the other key factor for microalgae growth, light, the improved design offer on average +4.3 % of sufficient light duration. This effect, while modest, is instructive. On the one hand, double-glazing and the greenhouse radiative selective film lower the amount of captured light. On the other hand, hosting a dilute culture (allowing 75 % of light to pass

through instead of 50 %) counterbalances these effects almost equally. Ultimately, light availability is maintained.

Figure 5 also delivers insights into the effect of inter-annum weather variations. The year 2013 exhibited low overall sun resources with reference and best configurations operating under low illumination most of the daytime (54 and 51.9 %, respectively). On the contrary, the year 2022 showed higher sun resources, with light-deficient fractions of the time being reduced to 43.3 and 40.9 %. This observation underlines the need to assess performances with actual meteorological data over multiple years, as discussed hereinafter.

Now that overall performances have been examined, the question of the role of the different parameters in performance improvement is to be addressed. Yet, this matter is complex, as interactions between the parameters could be at play. To sort it out, two indicators were calculated. The first one is the marginal improvement offered by one parameter. It represents the effect of this design parameter, given that all the others are already implemented. The second one is the basal improvement offered by one parameter. It represents the effect of this parameter alone when all the others have been kept at the reference level. Effect size and effect size indices of these two indicators are reported in Table 2. The marginal impact of all the design parameters is relatively high, most yielding an increase of the order of magnitude of hundreds of hours, with sizable Cohen's d value (above 0.8 for most). On the contrary, the basal effect of the parameters is relatively low (tens of hours, Cohen's d below 0.10), except for the reservoir thickness. This last parameter has a moderate negative effect at the basal level. The observed differences between marginal and basal effects of parameters (one even changing the sign of its contribution) point toward sizable interaction effects between the parameters. This aspect will be further investigated in a coming section.

Before moving to in-depth investigation of the parameters' main effects and interactions, year-to-year variation for reference and optimized configurations is the last element to examine. Figure 6 reports the distribution of the total yearly duration for which temperature and light are adequate. As one can see, it increases over the last decade for both configura-

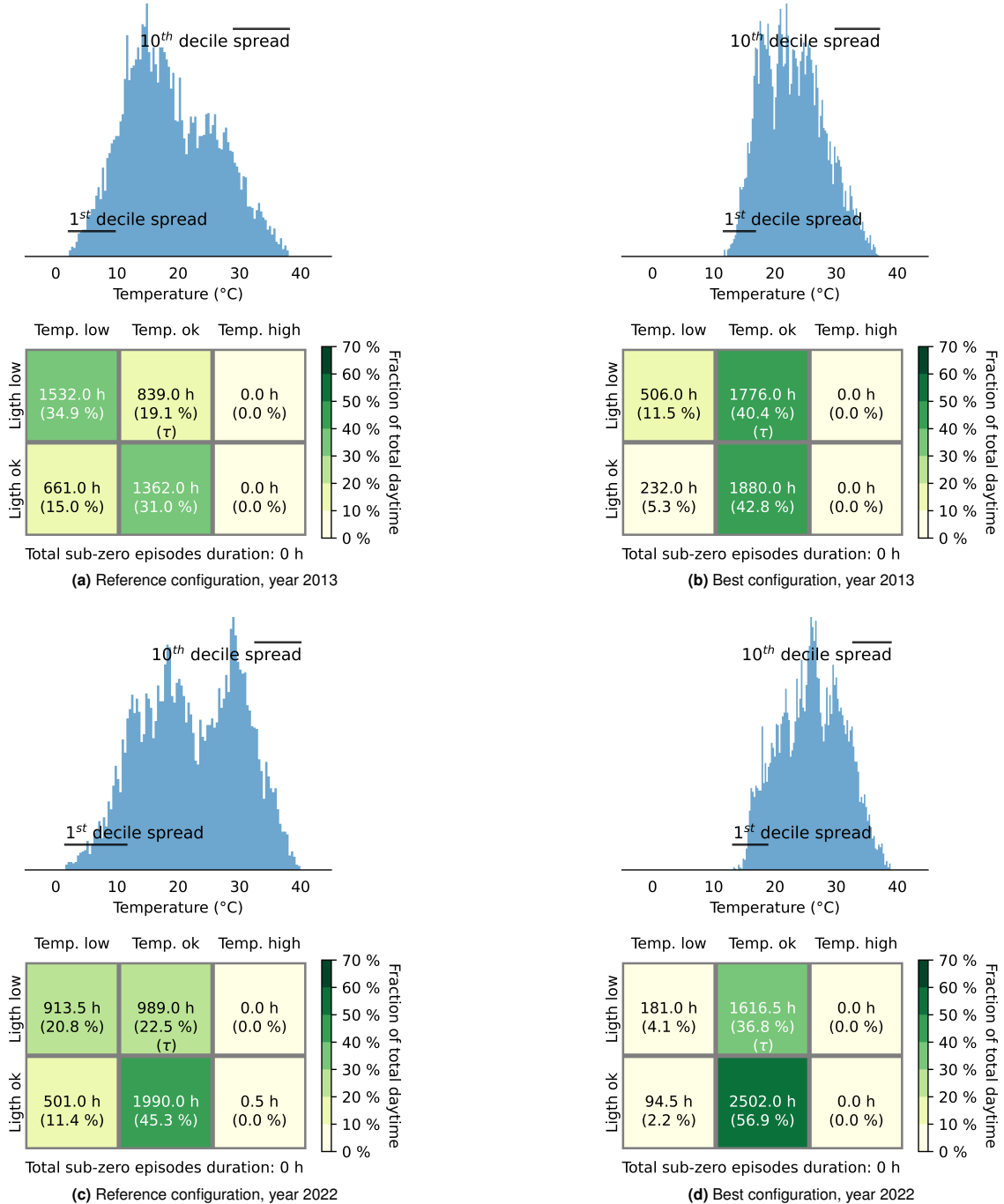


Fig. 5. Biofaçade performance indicators for the reference and the best configurations. For each subfigure: Top - temperature distribution over daytime (as frequency or number of occurrence over the year). Bottom - daytime operating hours repartition

tions, with a surge in 2015. This increase was quantified, using linear regression, to +41.5 h/year (95 % confidence interval ± 2.0 h/year) for best configuration and +41.3 h/year (95 % confidence interval ± 1.9 h/year) for reference one. Drawing the distribution also bears information on how the performances are affected by the uncertainty tied to some physical properties (*e.g.*, surrounding buildings' emissivity). As one can see, by going from the reference setup to the optimized one, the distribution gets skewed favorably to higher performances. This shows that, in addition to delivering improved

performances, the optimized design also delivers more robust performances.

4.2. Parameters main effect

This Section will deal with the main effect of each parameter. However, the vast nature of the dataset and the spread of the parameters' values do not ease interpretation. Furthermore, analyzing the differences between the reference and the best case suggested that sizable interactions might be at play. Therefore, parameters will be analyzed sequentially to progressively reduce the complexity by discarding the less

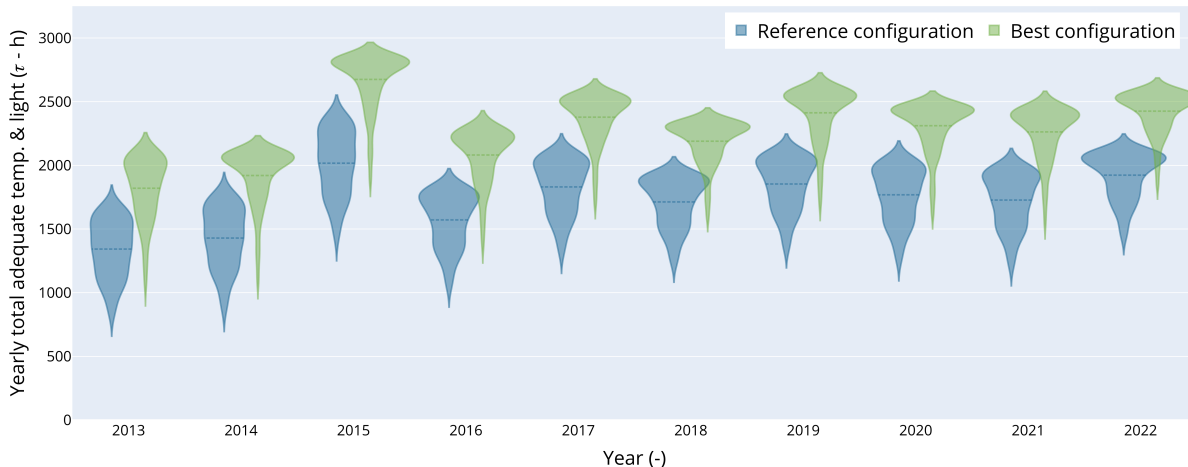


Fig. 6. Distributions of the number of hours for which both illumination and temperature are adequate for the reference and best configuration over the last 10 years. Location: Marseille, France

interesting combinations and disambiguating the parameters' main effects on the relevant ones. The first parameter to be reduced is the year over which performances are obtained. Indeed, Figure 6 showed that, as the climate gets warmer, biofaçade performances increase. Therefore, to limit the variability induced by this factor, the year 2018 will be selected to illustrate the following analyses.

4.2.1. Orientation. Figure 7 displays the distributions of the number of hours for which both illumination and temperature are adequate for the five tested orientations over the year 2018. As one can see, the distributions feature several modes and are quite dissembling. The only common parameter is their spread. Indeed, due East and due West are capped at around 1500 hours. Southeast and Southwest are capped at around 2000 hours. Due South orientation offers up to about 2400 hours of production time. As those distributions are different, one has to be chosen to carry on the analysis. Due South was chosen as it represents the most favorable case. Hence, it would surely represent the first intention from a technology deployment perspective.

Another detail is to be noted: the distributions display many configurations for which the total number of producible hours is null. Those configurations are born of the conjunction on inadequate design parameters combination (*e.g.* a thermophilic strain placed in a biofaçade with a large reservoir, no additional glazing, and a film limiting heat capture) and unfavorable draws of uncertain parameters (*e.g.*, high microalgae culture emissivity, further lowering the biofaçade temperature). Therefore, to limit the impact of obviously misconceived configurations, the dataset was further limited to the configurations achieving performances at least as good as the reference configuration (1717.6 h) on average over the 10-year simulated period.

4.2.2. Strain type. The performance distribution of biofaçade hosting the regular, mesophilic, strain (*Chlorella vulgaris*) and the thermophilic strain (*Chlorella sorokiniana*) are presented in Figure 8. As one can see, the thermophilic strain is substantially under-performing and the sole one producing

null performance values. Furthermore, applying the criterion introduced in the previous Section excludes all the runs for which *Chlorella sorokiniana* was chosen for the culture. It can therefore be concluded that, even in the South of France, a thermophilic strain is not adequate for a biofaçade system. Based on this conclusion, runs featuring the thermophilic strain were excluded from the dataset used for further analyzing the parameters' main effects.

4.2.3. Gasing strategies. Two strategies were envisioned regarding the gas sparged into the culture. The first was to either draw air from the building, lowering its emitted pollution, or from the outdoors, contributing to cleaning outdoor air. Figure 9, left, illustrates the effect of this choice on the performance distribution. Both options yield incredibly similar outputs. From the observation of the distribution, the air coming from the building would seem to be more advantageous. The distribution closeness makes them difficult to discriminate with certainty by the human eye. Computing Cohen's d index, it is possible to ascertain this feeling. The computation yields a value of 0.027. It can therefore be concluded that choosing air coming from the building has a negligible effect. Further analyses were led with air coming from the building.

The second strategy was to reuse fumes coming from the building boiler during wintertime. Two improvements were expected: increased culture temperature and increased carbon dioxide supply. Figure 9, right, shows the performance distribution of a biofaçade taking advantage of the boiler fumes versus the reference configuration. Reusing boiler fumes offers a slight improvement, from 1845.8 ± 221.6 hours to 1884.9 ± 210.5 hours. From a statistical point of view, it can be deemed minor, with a Cohen's d value of 0.17. However, one should note that only part of the benefits of this strategy could be assessed here (thermal boost). Using a finer biological model (account for CO₂ biofixation) could, perhaps, reinforce the relevance of this strategy.

From a modeling perspective, observing modest effects of the sparged gas manipulation strategies was anticipated in the

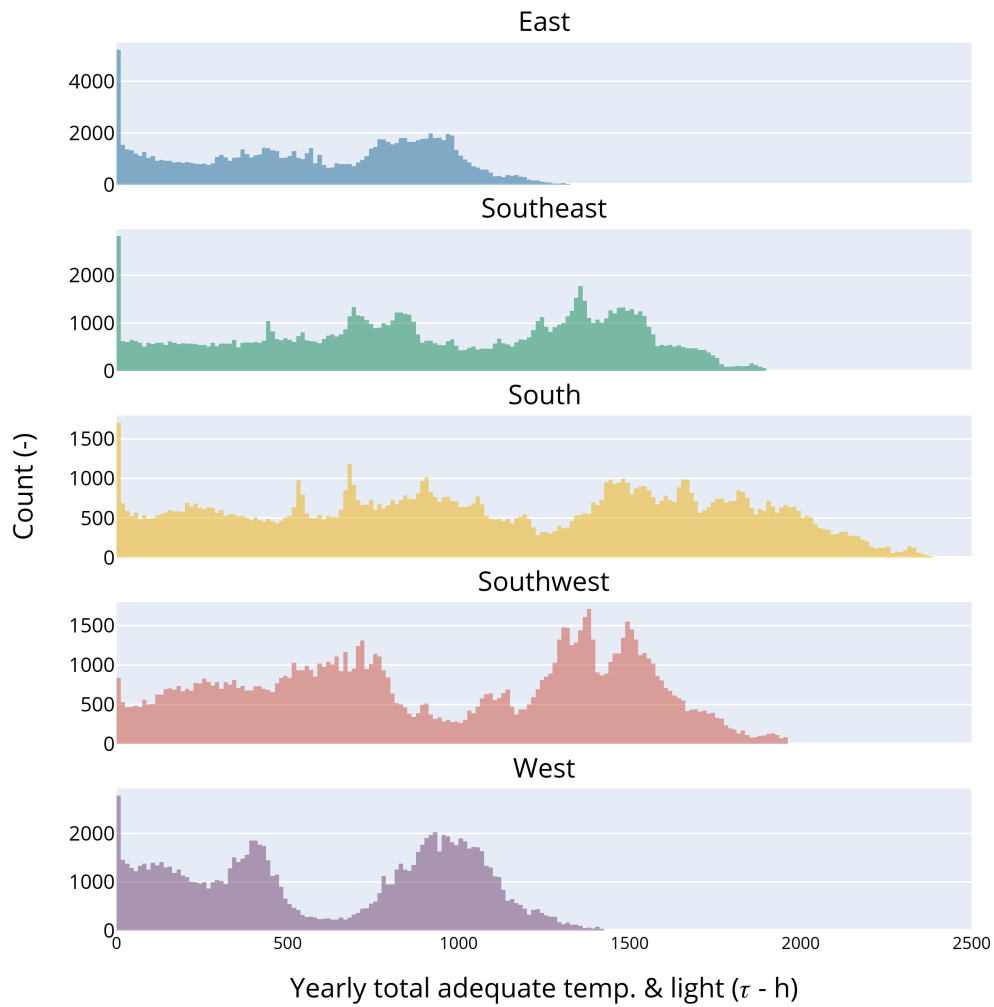


Fig. 7. Distributions of the number of hours for which both illumination and temperature are adequate. Year 2018. From top to bottom: East, Southeast, South, Southwest, West

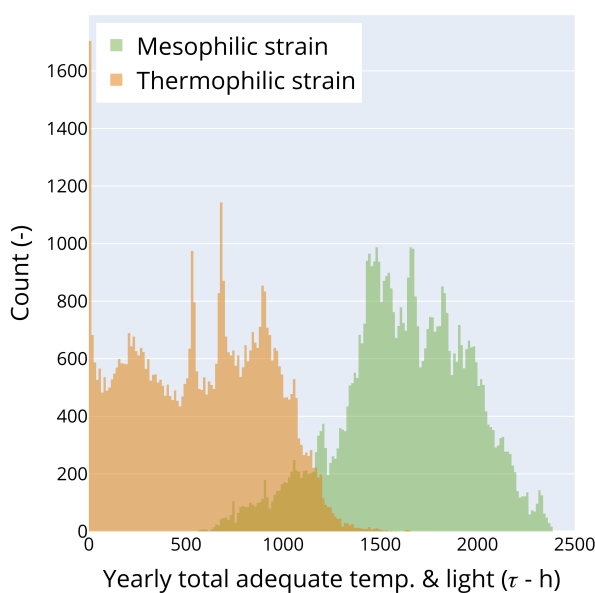


Fig. 8. Comparison of the distributions of the number of hours for which both illumination and temperature are adequate for the regular strain (*Chlorella vulgaris*) and the thermophilic strain (*Chlorella sorokiniana*). Year 2018, due South

companion article. Having it emerging from the data analysis is a token of the robustness of the deployed methodology. From a biofaçade conception perspective, air origin does not impact the system's performance. The choice could therefore boil down to a branding preference between cleaning the city air and limiting building pollution. Conversely, implementing a boiler fumes reuse strategy increases the system's performance but will surely represent a sizable cost as a dedicated piping system would have to be installed. Therefore, the choice of this strategy will have to be weight with care, and its relevance can only be argued by going beyond the scope of this work and including the environmental and financial dimensions. As our best configuration was obtained by implementing this last strategy, the analysis will be carried out assuming its implementation.

4.2.4. Heat capture strategies. Obtaining as much heat as possible without inducing overheating is paramount for a biofaçade to operate at its full potential. In this view, the use of double glazing to limit heat loss toward the surrounding was envisioned as a relevant option. Another modulation was the use of radiation-selective films to limit radiative heat loss (greenhouse film) or select visible incident light only (visi-

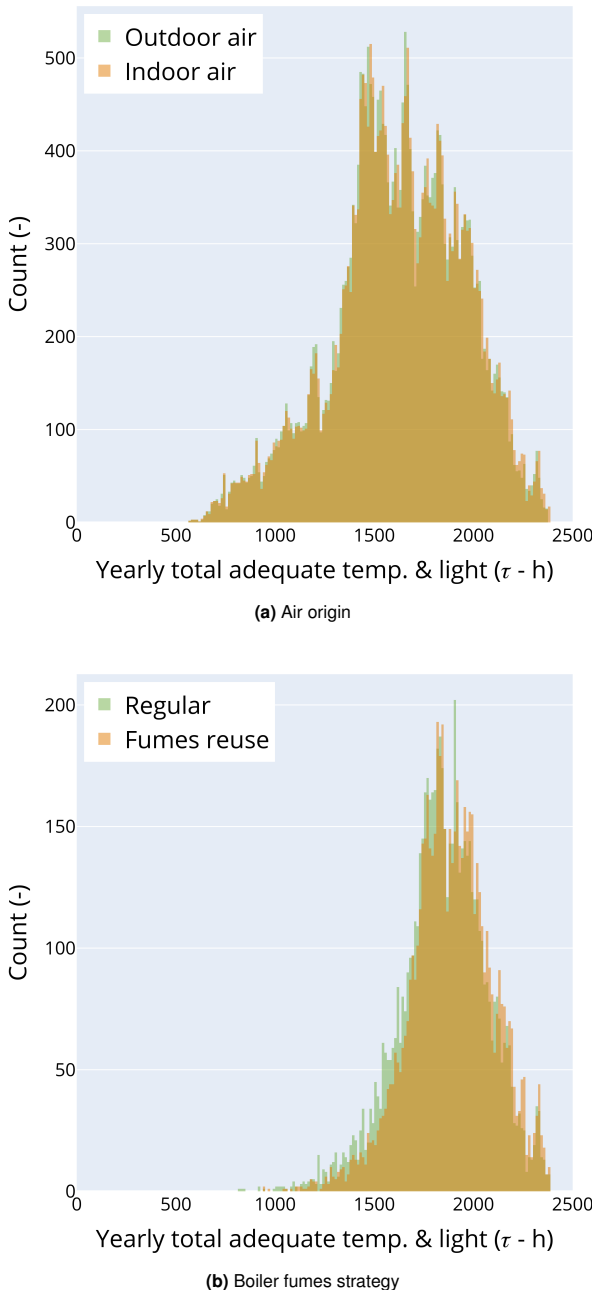


Fig. 9. Number of hours for which both illumination and temperature are adequate for the different gazing strategies. Year 2018, due South, *Chlorella vulgaris*

ble only film). Figure 10 left presents the adequate operation durations for the different combinations of these two parameters. The first comment is that disregarding the parameter combination drawn on the graph, the distributions exhibit a multi-modal shape (3 to 4 modes). The observed peaks originate from the two last design parameters that have not been discussed yet, and are the topic of the next Section: the culture reservoir thickness and the optical thickness. Nevertheless, some valid observations and conclusions can be drawn.

First, the film selecting visible and infrared radiations while limiting long wavelength radiation emission (tagged as greenhouse) outperforms the reference configuration and the visible-only film. It is explained by the fact that although it reduces the overall captured energy, limiting heat radiative emission provides a substantial benefit. This comment is also, in part, valid for the visible-only, which outperforms the reference configuration in the case of the use of double glazing.

Second, the overall effect of double glazing (green distributions) is to be analyzed. Resorting to double glazing systematically improves average and maximal performances. However, it not only shifts the distributions upwards but also spreads the distributions. This suggests that not all configurations benefit equally from the double-glazing installation. To understand this effect, one has to remind that fitting additional glazing is a double edge sword. On one side, it helps to keep the biofaçade temperature high (upward shifting). On the other, it induces additional reflections lowering the captured energy to some extent (downward spreading). This loss of visible light could be the reason why some configurations do not take full advantage of the additional heat harnessed by the double glazing. To confirm this hypothesis, the total number of adequate lighting hours (disregarding temperature levels) was compared between single and double-glazing configurations. Over the whole dataset, the loss of adequate lighting duration only represents a -1.2 % decrease. Focusing on the best-case scenario, it drops to -1.7 %. These figures are surprisingly low but can be explained both physically and biologically. Physically, fitting double glazing lowers the absorbed light by -4.2 % (low contrast of refraction index between PMMA and air and almost 100 % transmission of the PMMA in the visible spectrum (42)). Biologically, microalgae do not benefit from light above a given value (150 $\mu\text{molPhotonPAR/m}^2/\text{s}$, in our case, which corresponds to an incident solar heat flux of 32.6 W/m^2) (19, 20). Above this value, the cells safely regulate excess light but do not produce more biomass. Hence, limiting light supply above this threshold value does not hinder cell growth. Therefore, in terms of illumination, it can be concluded that double glazing does not affect a microalgae culture hosted in a biofaçade in a significant manner. While of high importance, this finding does not explain the observed modulation of the effect of the double glazing.

The explanation for the uneven effect of double glazing is to be found in the intrinsic capacity of the biofaçade to harvest heat. This capacity is influenced by some physical parameters, among which lie the ones with uncertainty asso-



Fig. 10. Left - Distributions of the total adequate operation duration as a function of the number of outdoor glazing (1 - blue, 2 - green) and radiation-selecting film. Year 2018, due South, *Chlorella vulgaris*. Right - Total temperature category shift (low to adequate and adequate to high) for each of the 256 runs by opting for a double glazing versus a single glazing. Reservoir thickness of 5 cm, no radiation-selective film, and light transmission of 50 %

ciated with their values (Sec. 2.5), *i.e.*, microalgae culture emissivity (ϵ_{mc}), building indoor emissivity (ϵ_{In}), and surrounding emissivity (ϵ_{Sur}). A high value of culture emissivity will foster heat loss, while high values of building indoor and surrounding emissivities will increase heat transferred to the biofaçade. Therefore, the different combinations of these parameters will influence double glazing efficiency. To disambiguate their combined effect, two metrics were calculated. The first one is the temperature displacement which represents how many hours went from too low to adequate and from adequate to high for a given configuration by shifting from a single glazing to a double glazing. The second is the heat harvesting potential, which aggregates the three parameters of interest. It is calculated as $\epsilon_{Sur} - \epsilon_{Sur,min} + \epsilon_{In} - \epsilon_{In,min} + \epsilon_{mc,max} - \epsilon_{mc}$. It ranges from 0 (most unfavorable configuration) to 0.6 (most favorable one). Figure 10 right presents the temperature displacement induced by adding supplementary glazing for a given design versus the heat harvesting potential. As one can see, the two variables show a clear upward correlation with a 13-fold increase between the worst and the best combinations. This observation reinforces the conclusion of the companion article: these three parameters are influential and correlated, with a known pattern and amplitude, now. Therefore, a finer assessment of their values appears mandatory to ascertain the performance prediction of foreseen design before its actual deployment.

Third, taking advantage of the fact that the model simulates a biofaçade with a sub-hourly resolution, the time of the year when double glazing is the most relevant was analyzed with the model. Figure 11 illustrates the temperature increase induced by double glazing for the year 2018. As one can see, the highest improvement is obtained over wintertime (about +4 °C during daytime, +8 °C during nighttime). This is especially beneficial and drives most of the gain in performance (+333 h of daytime adequate temperature over January to March and October to December over the +531.5 h for the whole year). During summertime, the temperature increase is more modest (+1 to +3 °C), which is explained by the higher solar altitude at this period of the year. Incidentally, it also reduces the risk of overheating. Finally, from a building performance perspective, fitting double glazing cuts the U-value from 6.32 to 1.23 W/m²/K.

Given the magnitude of the effect of resorting to double glazing, one may wonder if this improvement could be furthered by using high-performance double glazing. Hence, a double-glazing design with Xenon (thermal conductivity of 0.00565 W/m/K) instead of air was simulated. It resulted in +97.5 h for adequate temperature operation over the year 2018. While a proper economic analysis should confirm it, this 2.7 % increase in performance can be deemed modest. Indeed, this type of high-performance double glazing is commonly admitted to induce a substantial increase in system production cost.

4.2.5. Thermal inertia and optical thickness. The last parameters to investigate are the reservoir thickness, which controls thermal inertia, and the optical thickness, which con-

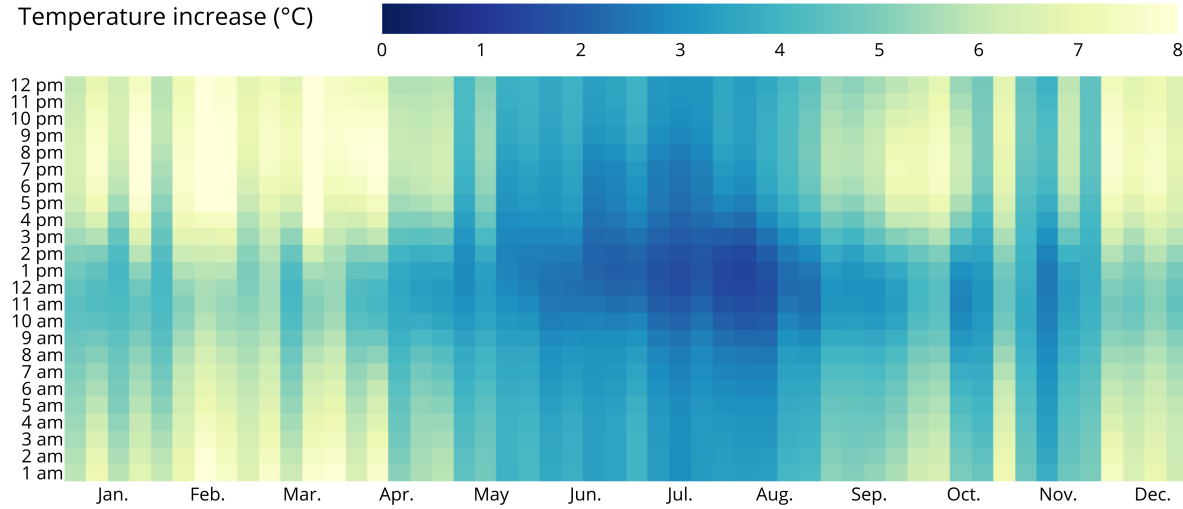


Fig. 11. Temperature increase induced by a double glazing (1 h daily time spans weekly averaged). Year 2018, due South, *Chlorella vulgaris*, reservoir thickness of 5 cm, greenhouse radiation-selective film, air from the building with boiler fumes reuse, and light transmission of 50 %

trols the amount of light passing through the culture. First of all, the data sub-setting procedure excluded too-dense cultures (only 25 % of light transmitted) and too-thin systems (2 cm deep reservoir). Figure 12 displays the biofaçade yearly adequate operation duration for the combination of the two values for the two parameters: 50 and 75 % of the light passing through and a 5 and 8 cm thick reservoir. As one can see, a larger reservoir systematically improves performance. This can be explained by the higher thermal inertia allowing to carry over energy from heat-sufficient periods (such as afternoons) to heat-deficient ones (such as evenings or cloudy episodes). This way, the microalgae can grow for an extended period compared to the reference configuration. This conclusion contradicts the finding of Barajas Ferreira *et al.* (5), who advised a narrow reservoir. However, as they pointed out, the temperature was constant at around 30 °C in their study, which prevented them from deciphering the relevance of the system's thermal inertia.

Regarding light, having a dilute culture also increases the microalgae favorable conditions. Indeed, lowering the culture concentration ensures a higher average illumination within the culture, hence a higher amount of light sufficient hours. Considering the building users' point of view, a dilute culture also limits the risk of too-dark moments, ensuring visual comfort (7). In this regard, Table 3 reports visual transmittance of the system for different optical thicknesses and the number of external glazing. First of all, absolute values are comparable to the ones reported by Ahamadi *et al.* (8). Then, one can see that the most influential factor is the optical thickness. Moreover, from a building perspective, manipulating the optical thickness allows the adjustment of the solar heat gain coefficient (Table 3), which behavior follows the one of visual transmittance. Nevertheless, from a process perspective, having a dilute is unfavorable, as it increases the cost of biomass harvesting. Therefore, this last observation

calls for additional elements before reaching a solid conclusion on microalgae culture concentration.

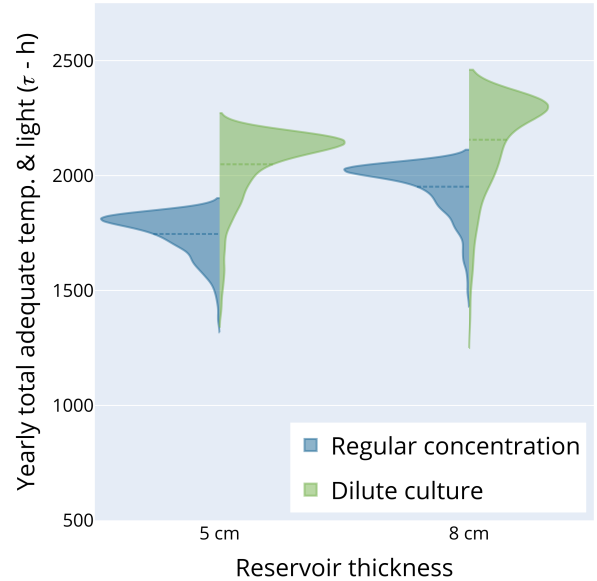


Fig. 12. Adequate operation yearly duration distributions for different reservoir thickness and light transmission. Year 2018, due South, *Chlorella vulgaris*, greenhouse radiation-selective film, air from the building with boiler fumes reuse

4.3. Location influence

Thanks to its wide temporal and spatial spread, the Météo-France dataset allows the simulation of microalgae biofaçade systems virtually anywhere in France. Therefore, to assess for location-based difference, the same procedure was led for another location than Marseille, *i.e.*, Paris. Paris was chosen as it hosts numerous tall buildings and represents a northerner place than Marseille, as well as an inland location (versus coastal for Marseille). Surprisingly, almost no difference

		Green light transmitted fraction (α)		
		0.25	0.5	0.75
Visual transmittance	Single	0.061	0.121	0.182
	Double glazing	0.058	0.116	0.174
Solar heat gain coefficient	Single	0.027	0.055	0.082
	Double glazing	0.026	0.053	0.079

Table 3. Visual transmittance and solar heat gain coefficient as a function of culture optical thickness, expressed as transmitted fraction of the green (500 to 600 nm) part of the visible spectrum, and number of external glazing

emerged from this location change. The optimal configuration is the same. The reference and optimal performances, over 10 years, are extremely close: 1712.8 ± 289.5 h per year versus 1717.6 ± 292.9 for the reference, and 2241.1 ± 310.0 h versus 2247.6 ± 313.6 for the optimal design. In addition to yielding very similar average values, changing the biofaçade location did not affect the spread around this value. This last indicator is essential as it materializes the robustness of the system and the stability versus year-to-year meteorological variations. Thus it can be concluded that the system performs in the same way in the two places. While surprising, this observation is very positive. Indeed, it opens the way towards system standardization, virtually cutting the production costs to equip large land areas with new systems. Nevertheless, it does not rule out the need for location-based optimization. Yet, the illumination and weather contrasts would have to be of a higher magnitude than the Marseille/Paris ones. Finally, in case of renovation, with inherent constraints, case-dependent optimization will have to be carried out, especially given the interplay between the design parameters.

4.4. Interaction between parameters

Analyzing design parameters' main effects yielded numerous insights into the thermal behavior of a microalgae biofaçade. However, it also unraveled part of the tremendous complexity at stake and pointed toward intense design parameter interactions. Several methods exist to investigate the interaction between variables. Some require rerunning a model, such as local sensitivity analysis (using derivatives) or global sensitivity analysis (e.g., Sobol's indices). Others have been designed to accommodate existing data. Among them, Friedman H^2 indices were chosen. Figure 13 presents H^2 indices for the biofaçade design parameters. On the right, the analysis was led on the whole dataset, including dramatically underperforming configurations. On the left, the analysis is restricted to the configurations performing at least as well as the reference design. The diagonal represents the overall interaction potential of a variable. The lower half represents the pairwise order 2 interactions (higher order could also be analyzed, though).

As one can see, on the whole dataset, four variables exhibit intense interactions, namely the number of glazing, the type of radiation-selecting film, the amount of transmitted light, and the culture reservoir thickness. This finding is not surprising given the observations drawn in the former section. Yet, it further highlights the complexity of optimizing the geometry of a biofaçade without having a holistic view of it and underlines the relevance of Umdu's design of experiment

approach (6). Finally, the type of strain is also a highly interactive parameter ($H^2 = 0.28$), but at an order higher than 2, as no substantial order 2 interactions are detected. Here again, the previous comments on the impact of the strain type (the thermophilic one yielding systematically poor results) explain this. While the left part of the Figure could be endlessly commented on, it accounts for irrelevant configurations for which in-depth analysis is not pertinent. It will therefore be halted here.

Moving on to the restricted dataset, one can see that the overall interaction potential of each parameter increases dramatically. For example, the number of glazing and the reservoir thickness have the two third of their effects mediated through interactions, representing a huge value. This interaction could be foreseen in Figure 10 (left) with the multimodal shape of the performance distributions. Furthermore, pairwise analysis shows that they are highly intertwined, but their interactions are also associated with other variables. In detail, variables interactions expand toward design/strategy interactions, with the fume reuse strategy exhibiting coupling effects, which were not evident on the whole dataset. Therefore, the conclusion is obvious: biofaçade design and operation strategy must be engineered together to exploit the full potential of the technology. On final comment is that, for the restricted dataset, the strain type interaction appears as null. It is expected, as only one strain type is present in this dataset. This observation is a token of the robustness of the H^2 metric.

4.5. Illustration case: optimizing a renovation

To illustrate the capability of the model, it was applied to the determination of the optimal design in the case of a hypothetical office building renovation. The building is located in Marseille, and the façade of interest is South-southwest oriented. As it is a renovation, some constraints apply. For example, the boiler fumes reuse strategy would be deemed too complex and costly to implement. In addition, the owner would like to claim that the system lowers building pollution. Hence the air would come from the building and not the outdoors. Finally, *Chlorella vulgaris* strain (mesophilic) was chosen, as previous analyses showed that the thermophilic strain would be irrelevant. Thus, the parameters to be optimized are the reservoir thickness, the number of glazing, the fraction of transmitted green light, and the type of radiative film, if any. Table 4 presents the resulting candidate space and the associated constraints on the parameters. As one can see, the possible reservoir thickness was extended up to 15 cm. The underlying idea was to investigate if there is a limit above which a larger reservoir would become unfavorable.

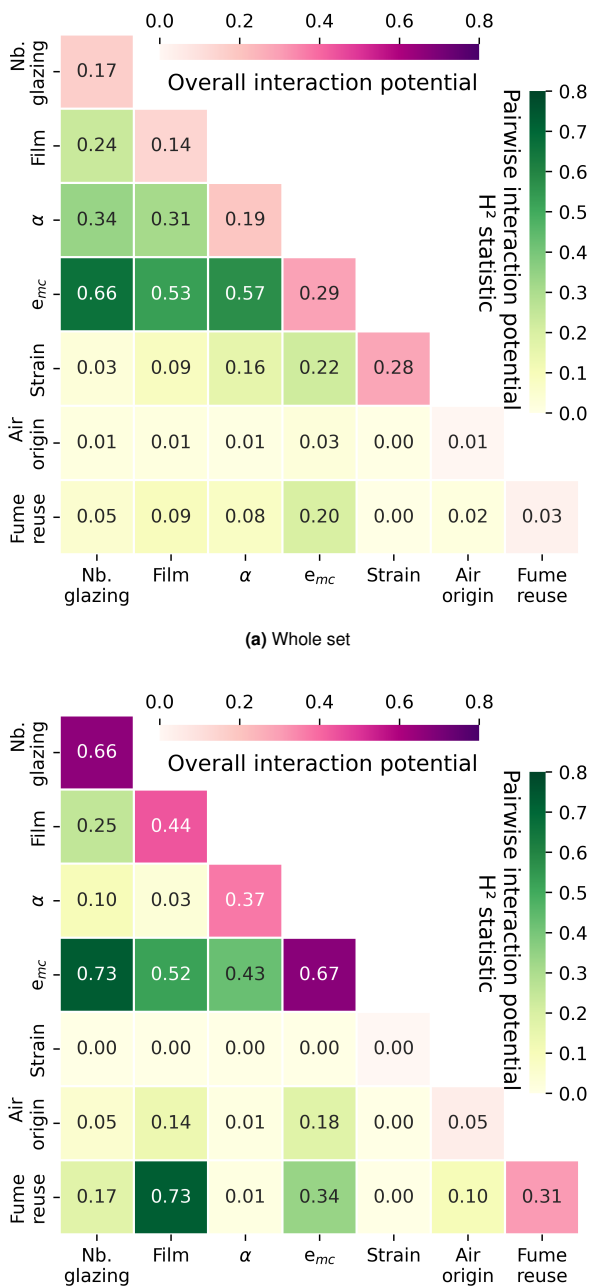


Fig. 13. Design parameter H^2 Friedman indices. Diagonal - overall interaction potential. Lower half - pairwise order 2 interactions. α - Transmitted light. e_{mc} - Culture reservoir thickness. Regression model: Random Forest, until pure leaves are obtained (43). Year 2018.

The output criterion to be optimized (Eq. 4) was set to be the number of adequate operating hours over the last 10 years (last part of the equation) while ensuring no overheating (first part of the equation) or sub-zero episodes (second part of the equation). More complex metrics, for example, accounting for year-to-year variation, of favoring production during specific periods of the year could also have been engineered. Instead, a relatively unsophisticated one was preferred for the sake of simplicity.

After defining a metric, the question of the choice of the optimizer itself has to be addressed. Given that the candidate space features both continuous (*i.e.*, e_{ms} and α) and categorical parameters (*i.e.*, the number of glazing or film type) gradient-based methods do not seem appropriate. In this type of configuration, stochastic methods have been shown to be more adequate. Among them, Particle Swarm Optimization is of note (44), as it is rather easy to implement and deploy on a parallel architecture, capable of browsing considerable candidate spaces even when facing discontinuous fitness functions. To do so, this algorithm mimics animal group exploration patterns. In a nutshell, each particle has its own exploration trajectory (inertia parameter), which is modulated by information exchange with the other members of the group (social parameter) and its own history (cognitive parameter) (45). Its versatility allows it to cover a wide range of applications from chemometrics to domestic thermal solar setup sizing (46, 47). Its main drawback comes from the social nature of the swarm which lead to premature convergence into a local optimum (one particle attracting the others to it). To avoid this pitfall, Particle Swarm Optimization can be coupled with another stochastic optimization method: Genetic Algorithms. Together, these optimization techniques form an adequate tool to solve the problem at hand (48). The optimization algorithm parameters were set as follows: 96 particles/exemplars, cognitive and social parameters of the swarm were both set to 0.6, the inertia followed a random chaotic model, and the mutation probability was set to 0.1. In addition, the maximum particle stagnation before entering a tournament was set to 15, and the tournament size to 0.2. Runs were stopped after the swarm's best particle stagnated for 20 iterations. For a detailed practical implementation, the interested reader is referred to the following article and the freely accessible repository associated with it (46).

$$\begin{aligned}
 f = & \left(\sum_{10 \text{ years}} (T_i > 39.9^\circ C) = 0 \right) \times \left(\sum_{10 \text{ years}} (T_i < 0^\circ C) = 0 \right) \\
 & \times \left(\sum_{10 \text{ years}} ((17.7 < T_i < 39.9^\circ C) \times (\bar{T}_i > 150 \mu\text{mol Photon/m}^2/\text{s})) \right)
 \end{aligned} \tag{4}$$

After a few iterations, the swarm converges to a unique global maximum (qualitatively assessed by drawing the candidate space from the swarm exploration). The resulting configuration is a biofaçade with double glazing, a greenhouse radiation-selective film, a reservoir of 15 cm, and a light transmission of 65 %. The system performances in the year

Parameter	Range	Unit
Thickness of the biofaçade reservoir (e_{mc})	[0.02, 0.15]	m
Number of outdoor glazing	1 or 2	-
Green light transmitted fraction (α)	[0.20, 0.80]	-
Radiative film type	None, Greenhouse, Visible-only	-

Table 4. Candidate space description. Algorithm used for the optimization: Particle Swarm Optimizer hybridized with a Genetic Algorithm with 96 particles, cognitive parameter of 0.6, social parameter of 0.6, with fuzzy inertia, mutation probability of 0.1, maximum particle stagnation before entering a tournament of 15, tournament size of 0.2, best value stagnation to stop the search of 20

2018 are displayed in Figure 14. As one can see, the biofaçade temperature distribution resembles the one of the best system in Section 3. The same is true for the overall performance (2118 hours over the year 2018 versus 2172 h for the best system facing South). Nevertheless, the increased reservoir thickness reduces the episodes during which the temperature is too cold. From the swarm behavior, it can even be inferred that a larger reservoir would be even more beneficial. However, at some point, it will represent a problem in terms of building static load and volume of culture medium to prepare to grow the microalgae. This last comment also highlights the limitation of the model as, ultimately, financial and environmental assessments will be needed to argue for the relevance of technical suggestions.

5. Limitations

While it allows to disambiguate the contribution of key elements that together design a microalgal biofaçade system, the proposed model needs to be validated experimentally before being deemed robust enough to be applied to fine-tuning biofaçade conception. For example, visual transmittance and solar heat gain coefficient, two essential characteristics of a glazing system, have been computed. Building a prototype of a module would allow to assess to which extent a manufacturing process deviates from the idealized configuration. In the same manner, indoor temperature was assumed to be constant over the whole year. While this power exchange is not dominant during the day, it is one that prevents the biofaçade temperature from dropping too low at night and, consequently, helps to minimize the thermal lag the following day. Therefore, accounting for indoor temperature modulation (based on occupancy) could improve the predictions. All these limitations call for a field trial of the technology in order to fine-tune numerical tools, rendering them able to advise on the relevance of a given design for a given building configuration.

6. Conclusion

This article explored the design of microalgae biofaçade thanks to a numerical model describing the system's thermal and biological behavior. Design options and operation

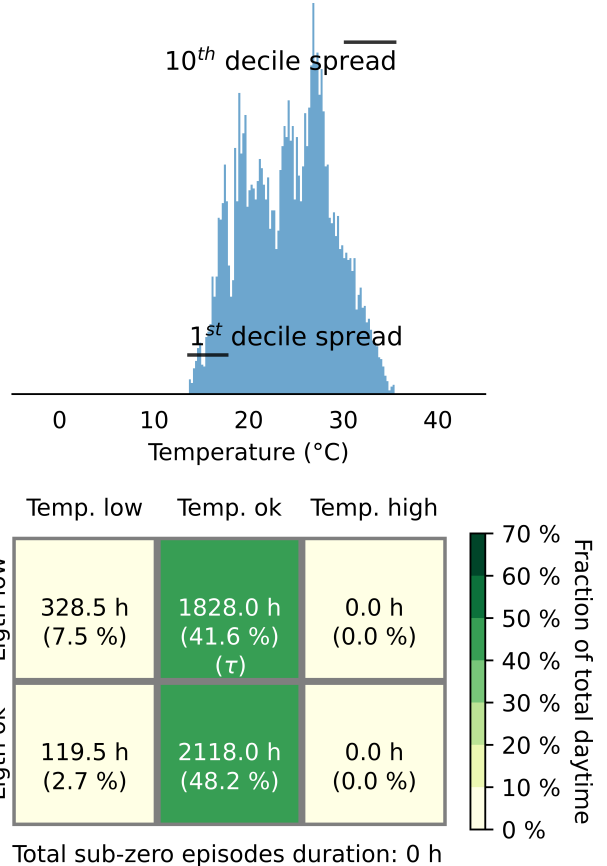


Fig. 14. Biofaçade performance indicators for the optimally designed system in the illustration case

strategies were screened systematically over a 10-year period (2013 to 2022) for which detailed meteorological data were available (air temperature, wind velocity and orientation, cloud cover, at a 3-hour resolution). These investigations revealed the very high level of interaction between the parameters, making the system notoriously complicated to design and optimize. Nevertheless, some conclusions can be drawn. In France, fitting double glazing equipped with a greenhouse film is essential to harness as much heat as possible (+16.7 % and +6.5 % of operating over year 2018, for example). Similarly, a thermophilic strain is not relevant because overheating events are nonexistent in well-designed systems. Further refinements, such as the origin of the air blown into the culture reservoir and the reuse of combustion fumes from the boiler (+2.1 % performance), can be evaluated from a technical point of view. However, their implementation would also be subjected to other considerations, such as the cost and environmental benefits. Furthermore, comparing two locations in France (Marseille and Paris) indicated that the optimal system shows low sensitivity to the location (at least for a 750 km distance). This fact opens the way for producing standard modules that could be fitted on new buildings. On the contrary, for already existing buildings, a location-specific optimization will always be needed to account for individual constraints. Thus the model was successfully applied to optimize a microalgae biofaçade system in the case of a hypothetical official building renovation. As

perspectives, this work calls for its extension towards three directions: life cycle analysis, biological model refinement, and experimental validation.

7. Model availability

A Python implementation of the proposed model is freely available at <https://github.com/victorpozzobon/biofacade>

Acknowledgements

Communauté urbaine du Grand Reims, Département de la Marne, Région Grand Est and European Union (FEDER Champagne-Ardenne 2014-2020) are acknowledged for their financial support to the Chair of Biotechnology of Centrale-Supélec and the Centre Européen de Biotechnologie et de Bioéconomie (CEBB).

Bibliography

1. Muhammad Rizwan, Ghulam Mujtaba, Sheraz Ahmed Memon, Kisay Lee, and Nain Rashid. Exploring the potential of microalgae for new biotechnology applications and beyond: A review. *Renewable and Sustainable Energy Reviews*, 92:394–404, September 2018. ISSN 1364-0321. .
2. Wendie Levasseur, Patrick Perré, and Victor Pozzobon. A review of high value-added molecules production by microalgae in light of the classification. *Biotechnology Advances*, 41:107545, July 2020. ISSN 0734-9750. .
3. Maryam Talaei, Mohammadjavad Mahdavinejad, and Rahman Azari. Thermal and energy performance of algae bio-reactive façades: A review. *Journal of Building Engineering*, 28: 101011, March 2020. ISSN 2352-7102. .
4. Rewaa Mahrous, Emanuela Giancola, Ahmed Osman, Takashi Asawa, and Hatem Mahmoud. Review of key factors that affect the implementation of bio-reactive façades in a hot arid climate: Case study north Egypt. *Building and Environment*, 214:108920, April 2022. ISSN 0360-1323. .
5. Crisóstomo Barajas Ferreira, Lucero Castro Padilla, Ginna Vanegas Sánchez, Angel Dario González-Delgado, and andres F. Barajas Solano. Design of a microalgae bio-reactive facade reactor for cultivation of Chlorella vulgaris. *Contemporary Engineering Sciences*, 10 (22 (2017)):1067–1074, November 2017. . Accepted: 2021-12-01T16:34:12Z Publisher: Contemporary Engineering Sciences.
6. Emin Selahattin Umdü, İlker Kahraman, Nurdan Yıldırım, and Levent Bilir. Optimization of microalgae panel bioreactor thermal transmission property for building façade applications. *Energy and Buildings*, 175:113–120, September 2018. ISSN 0378-7788. .
7. Hanieh Sarmadi and Mohammadjavad Mahdavinejad. A designerly approach to Algae-based large open office curtain wall Façades to integrated visual comfort and daylight efficiency. *Solar Energy*, 251:350–365, February 2023. ISSN 0038-092X. .
8. Ferial Ahmadi, Sara Wilkinson, Hamidreza Rezazadeh, Suraparb Keawwasvong, Qodsiye Najafi, and Arash Masoumi. Energy efficient glazing: A comparison of microalgae photobioreactor and Iranian Orosi window designs. *Building and Environment*, 233:109942, April 2023. ISSN 0360-1323. .
9. Jan Wurni and Martin Pauli. SolarLeaf: The world's first bio-reactive façade. *arq: Architectural Research Quarterly*, 20(1):73–79, March 2016. ISSN 1359-1355, 1474-0516. . Publisher: Cambridge University Press.
10. Ines Wagner, Christian Steinweg, and Clemens Posten. Mono- and dichromatic LED illumination leads to enhanced growth and energy conversion for high-efficiency cultivation of microalgae for application in space. *Biotechnology Journal*, 11(8):1060–1071, 2016. ISSN 1860-7314. . eprint: <https://onlinelibrary.wiley.com/doi/pdf/10.1002/biot.201500357>.
11. Robert Dillschneider, Christian Steinweg, Rosa Rosello-Sastre, and Clemens Posten. Biofuels from microalgae: Photoconversion efficiency during lipid accumulation. *Bioresource Technology*, 142:647–654, August 2013. ISSN 0960-8524. .
12. Arthur Oliver, Cristobal Camarena-Bernard, Jules Lagirarde, and Victor Pozzobon. Assessment of Photosynthetic Carbon Capture versus Carbon Footprint of an Industrial Microalgal Process. *Applied Sciences*, 13(8):5193, January 2023. ISSN 2076-3417. . Number: 8 Publisher: Multidisciplinary Digital Publishing Institute.
13. Thijs Defraeye and Jan Carmeliet. A methodology to assess the influence of local wind conditions and building orientation on the convective heat transfer at building surfaces. *Environmental Modelling & Software*, 25(12):1813–1824, December 2010. ISSN 1364-8152. .
14. Recommended Practice for the Calculation of Daylight Availability. *Journal of the Illuminating Engineering Society*, 13(4):381–392, July 1984. ISSN null. . Publisher: Taylor & Francis .eprint: <https://doi.org/10.1080/00994480.1984.10748791>.
15. Thomas D. Brock. Life at High Temperatures. *Science*, 230(4722):132–138, October 1985. ISSN 0036-8075, 1095-9203. .
16. Victor Pozzobon, Wendie Levasseur, Elise Viau, Emilie Michiels, Tiphaine Clément, and Patrick Perré. Machine learning processing of microalgae flow cytometry readings: illustrated with Chlorella vulgaris viability assays. *Journal of Applied Phycology*, 32(5):2967–2976, October 2020. ISSN 1573-5176. .
17. Olivier Bernard and Barbara Rémond. Validation of a simple model accounting for light and temperature effect on microalgal growth. *Bioresource Technology*, 123:520–527, November 2012. ISSN 0960-8524. .
18. Carl Safi, Bachar Zebib, Othmane Merah, Pierre-Yves Pontalier, and Carlos Vaca-Garcia. Morphology, composition, production, processing and applications of Chlorella vulgaris: A review. *Renewable and Sustainable Energy Reviews*, 35:265–278, July 2014. ISSN 1364-0321. .
19. Jörg Degen, Andrea Uebel, Axel Retze, Ulrike Schmid-Staiger, and Walter Trösch. A novel airlift photobioreactor with baffles for improved light utilization through the flashing light effect. *Journal of Biotechnology*, 92(2):89–94, December 2001. ISSN 0168-1656. .
20. Wendie Levasseur, Patrick Perré, and Victor Pozzobon. Chlorella vulgaris acclimated cultivation under flashing light: An in-depth investigation under iso-actinic conditions. *Algal Research*, 70:102976, March 2023. ISSN 2211-9264. .
21. Victor Pozzobon. Chlorella vulgaris cultivation under super high light intensity: An application of the flashing light effect. *Algal Research*, 68:102874, November 2022. ISSN 2211-9264. .
22. Thomas Huld, Elena Paietta, Paolo Zangheri, and Irene Pinedo Pascua. Assembling Typical Meteorological Year Data Sets for Building Energy Performance Using Reanalysis and Satellite-Based Data. *Atmosphere*, 9(2):53, February 2018. ISSN 2073-4433. . Number: 2 Publisher: Multidisciplinary Digital Publishing Institute.
23. I. M. Sobol. On the distribution of points in a cube and the approximate evaluation of integrals. *USSR Computational Mathematics and Mathematical Physics*, 7(4):86–112, January 1967. ISSN 0041-5553. .
24. Adham M. Elmalky and Mohamad T. Araji. Computational fluid dynamics using finite volume method: A numerical model for Double Skin Façades with renewable energy source in cold climates. *Journal of Building Engineering*, 60:105231, November 2022. ISSN 2352-7102. .
25. Adham M. Elmalky and Mohamad T. Araji. Multi-objective problem of optimizing heat transfer and energy production in algal bioreactive façades. *Energy*, 268:126650, April 2023. ISSN 0360-5442. .
26. Emeka G. Nwoba, David A. Parlevliet, Damian W. Laird, Kamal Alameh, and Navid R. Moheimani. Sustainable phycocyanin production from *Arthrospira platensis* using solar-control thin film coated photobioreactor. *Biochemical Engineering Journal*, 141:232–238, January 2019. ISSN 1369-703X. .
27. Rémi Waché, Tim Fielder, Will E. C. Dickinson, Joe L. Hall, Peter Adlington, Stephen J. Sweeney, and Steven K. Clowes. Selective light transmission as a leading innovation for solar swimming pool covers. *Solar Energy*, 207:388–397, September 2020. ISSN 0038-092X. .
28. Carla Balocco, Luca Mercatelli, Niccolò Azzali, Marco Meucci, and Giuseppe Grazzini. Experimental transmittance of polyethylene films in the solar and infrared wavelengths. *Solar Energy*, 165:199–205, May 2018. ISSN 0038-092X. .
29. Qiang Gao, Xiaomei Wu, and Dongming Wang. Effect of fluorine and niobium co-doping on boosting the NIR blocking performance of TiO2 nanoparticles for energy efficient window. *Solar Energy*, 238:60–68, May 2022. ISSN 0038-092X. .
30. F. Fasaei, J. H. Bitter, P. M. Siegers, and A. J. B. van Boxtel. Techno-economic evaluation of microalgae harvesting and dewatering systems. *Algal Research*, 31:347–362, April 2018. ISSN 2211-9264. .
31. Humberto J. Silva and S. John Pirt. Carbon Dioxide Inhibition of Photosynthetic Growth of Chlorella. *Microbiology*, 130(11):2833–2838, 1984. ISSN 1465-2080. . Publisher: Microbiology Society.
32. Clara Serrano, Henar Portero, and Esperanza Monedero. Pine chips combustion in a 50kW domestic biomass boiler. *Fuel*, 111:564–573, September 2013. ISSN 0016-2361. .
33. Jun Li, Kehou Pan, Xueqi Tang, Yun Li, Baohua Zhu, and Yan Zhao. The molecular mechanisms of Chlorella sp. responding to high CO2: A study based on comparative transcriptome analysis between strains with high- and low-CO2 tolerance. *Science of The Total Environment*, 763:144185, April 2021. ISSN 0048-9697. .
34. Aloice W. Mayo. Effects of temperature and pH on the kinetic growth of unicellular Chlorella vulgaris cultures containing bacteria. *Water Environment Research*, 69(1):64–72, 1997. ISSN 1554-7531. . eprint: <https://onlinelibrary.wiley.com/doi/pdf/10.2175/106143097X125191>.
35. Constantine Sorokin and Robert W. Krauss. Effects of Temperature & Illuminance on Chlorella Growth Uncoupled From Cell Division. *Plant Physiology*, 37(1):37–42, January 1962. ISSN 0032-0889. .
36. Hamidreza Rezazadeh, Zahra Salashroo, Ferial Ahmadi, and Farshad Nasrollahi. Reduction of carbon dioxide by bio-façades for sustainable development of the environment. *Environmental Engineering Research*, 27(2), 2022. ISBN: 1226-1025 Publisher: Korean Society of Environmental Engineers.
37. Gail M. Sullivan and Richard Feinn. Using Effect Size—or Why the P Value Is Not Enough. *Journal of Graduate Medical Education*, 4(3):279–282, September 2012. ISSN 1949-8349. .
38. Dongsheng Yang and Jarrod E. Dalton. A unified approach to measuring the effect size between two groups using SAS. In *SAS global forum*, volume 335, pages 1–6. Citeseer, 2012. .
39. Jerome H. Friedman and Bogdan E. Popescu. Predictive learning via rule ensembles. *The Annals of Applied Statistics*, 2(3):916–954, September 2008. ISSN 1932-6157, 1941-7330. . Publisher: Institute of Mathematical Statistics.
40. Lucian Părvulescu, Claudia Zaharia, Alina Satmari, and Lucian Drăguț. Is the distribution pattern of the stone crayfish in the Carpathians related to karstic refugia from Pleistocene glaciations? *Freshwater Science*, 32(4):1410–1419, December 2013. ISSN 2161-9549. . Publisher: The University of Chicago Press.
41. Natacha Motisi, Fabienne Ribeyre, and Sylvain Poggi. Coffee tree architecture and its interactions with microclimates drive the dynamics of coffee berry disease in coffee trees. *Scientific Reports*, 9(1):2544, February 2019. ISSN 2045-2322. . Number: 1 Publisher: Nature Publishing Group.
42. Xioning Zhang, Jun Qiu, Xingcan Li, Junming Zhao, and Linhua Liu. Complex refractive indices measurements of polymers in visible and near-infrared bands. *Applied Optics*, 59 (8):2337, March 2020. ISSN 1559-128X, 2155-3165. .
43. Fabian Pedregosa, Gaël Varoquaux, Alexandre Gramfort, Vincent Michel, Bertrand Thirion, .

- Olivier Grisel, Mathieu Blondel, Peter Prettenhofer, Ron Weiss, Vincent Dubourg, Jake Vanderplas, Alexandre Gramfort, David Cournapeau, Matthieu Brucher, Matthieu Perrot, and Édouard Duchesnay. Scikit-learn: Machine Learning in Python. *Journal of Machine Learning Research*, 12(Oct):2825–2830, 2011. ISSN 1533-7928.
44. Federico Marini and Beata Walczak. Particle swarm optimization (PSO). A tutorial. *Chemometrics and Intelligent Laboratory Systems*, 149:153–165, December 2015. ISSN 0169-7439. .
45. R. Eberhart and J. Kennedy. A new optimizer using particle swarm theory. In *MHS'95. Proceedings of the Sixth International Symposium on Micro Machine and Human Science*, pages 39–43, October 1995. .
46. Victor Pozzobon, Wendie Levasseur, Cédric Guerin, and Patrick Perré. Nitrate and nitrite as mixed source of nitrogen for Chlorella vulgaris: fast nitrogen quantification using spectrophotometer and machine learning. *Journal of Applied Phycology*, March 2021. ISSN 1573-5176. .
47. Raffaele Bornatico, Michael Pfeiffer, Andreas Witzig, and Lino Guzzella. Optimal sizing of a solar thermal building installation using particle swarm optimization. *Energy*, 41(1):31–37, May 2012. ISSN 0360-5442. .
48. Y. Gong, J. Li, Y. Zhou, Y. Li, H. S. Chung, Y. Shi, and J. Zhang. Genetic Learning Particle Swarm Optimization. *IEEE Transactions on Cybernetics*, 46(10):2277–2290, October 2016. ISSN 2168-2267. .